sustainability

MDPI

Article

Analysis of Pressure Fluctuation of Tubular Turbine under Different Application Heads

Yaping Zhao [1], Jianjun Feng [1,*], Zhihua Li [1,2], Mengfan Dang [1] and Xingqi Luo [1]

[1] Institute of Water Resources and Hydropower, Xi'an University of Technology, Xi'an 710048, China; zyp0168@xaut.edu.cn (Y.Z.); lizhihua@tpri.com.cn (Z.L.); dang13720651376@163.com (M.D.); luoxq@xaut.edu.cn (X.L.)

[2] Xi'an Thermal Power Research Institute Co., Ltd., Xi'an 710054, China

* Correspondence: jianjunfeng@xaut.edu.cn

Abstract: The vigorous development of low-head hydraulic resources and tidal energy with greater stability and predictability is drawing attention to tubular turbines. However, many problems, such as incorrect unit association relationship, insufficient unit output, and severe vibration, occur frequently in tubular turbines, particularly when the water head is low. These phenomena cannot be known through model machine tests and numerical studies. Therefore, this study takes the tubular turbine with different water heads as the research object, in accordance with the actual boundary conditions. The unsteady numerical research for the prototype machine is conducted while considering the free surface in the reservoir area and water gravity. The internal flow characteristics of the tubular turbine with different water heads and the influence of free surface on its performance are analyzed. The research indicates the following: affected by the free surface and the water gravity, the pressure in the entire flow passage of the horizontal tubular turbine increases with the increase in the submerged depth. In addition, the short water diversion section allows the water flow from the reservoir area to still have a certain asymmetry before reaching the runner. During the rotation process of the runner, the surface pressure and torque of the blade have evident periodic fluctuations, and the amplitude of the fluctuations will increase significantly with the decrease in H/D_1. Moreover, in the case of small H/D_1, the amplitude of pressure pulsation in the draft tube is larger, and concentrated high-frequency pressure pulsation occurs. These factors will lead to the occurrence of material fatigue damage, unstable output, and increased vibration in low-head tubular turbines.

Keywords: tubular turbine; H/D_1; numerical analysis; pressure pulsation

Citation: Zhao, Y.; Feng, J.; Li, Z.; Dang, M.; Luo, X. Analysis of Pressure Fluctuation of Tubular Turbine under Different Application Heads. *Sustainability* **2022**, *14*, 5133. https://doi.org/10.3390/su14095133

Academic Editors: Zhengmao Li, Tianyang Zhao, Ke Peng, Jinyu Wang, Zao Tang, Sumedha Sharma and Majid Mohammadian

Received: 2 March 2022
Accepted: 22 April 2022
Published: 24 April 2022

1. Introduction

In recent years, the development of ultra-low-head hydraulic resources and tidal energy with greater stability and predictability has attracted much attention. In addition, the tubular turbine is widely used for its evident advantages in the development of extra-large flow, ultra-low-head hydraulic resources, and tidal energy. As its performance and structure are different from those of conventional vertical shaft units, domestic and foreign scholars conducted considerable work on research methods and technical means through numerical simulation and model tests. Focusing on the analysis of special flow phenomena (e.g., clearance flow and cavitation characteristics) of tubular turbines and the improvement of energy characteristics [1–3], several studies have been carried out on the energy characteristics, cavitation characteristics, vibration characteristics, and optimal design of tubular turbines [4–6]. Particularly, the hydraulic vibration of the turbine and the fatigue damage of the unit's structural components caused by the hydraulic vibration have attracted much attention [7–9]. At present, the problem of stress distribution, vibration deformation, and material fatigue damage of overcurrent components is mainly solved through fluid–structure coupling, and good research results have been achieved [10,11]. These studies greatly improved the overall performance of the tubular turbine.

However, the operation of many power stations shows that many problems, such as incorrect unit association relationship, damage to overflow components caused by cavitation [12,13], insufficient unit output, and severe vibration, frequently occur during the operation of ultra-low-head tubular power stations. In particular, severe vibration is an important factor limiting the safe operation of ultra-low-head tubular turbines. Thus, the power station has to limit the operating range of the unit to avoid severe vibration [14]. This study investigates the reasons for its severe vibration. In addition to factors such as hydraulic imbalance common to conventional power plants, low-frequency pressure pulsation in draft tubes, cavity cavitation, Karman vortex trains, and interstitial jets, factors unique to ultra-low-head tubular units also exist. Such factors are manifested in the following aspects: (1) The hydrostatic pressure difference generated by the gravity of the water makes the blade always experience a periodic cycle process of high pressure–low pressure–high pressure [15,16]. Moreover, a single blade rotates around the shaft to experience torque changes, forming periodic torque disturbances and causing dynamic oscillations, leading to blade cracks in severe cases [17,18]. (2) The hydrostatic pressure difference caused by the gravity of the water inside the tubular turbine makes the cavitation in the runner mainly concentrated at the top [19], and periodic cavitation is formed with the periodic change in position during the rotation of the blade that has occurred during cavitation. In addition, the pressure pulsation generated by the jet in the gap on the blade end face will experience high to low pressure with the rotation of the unit. The changes and the formation of periodic pressure pulsation can induce vibration of the unit. (3) The hydrostatic pressure difference in the tubular turbine affects the hydraulic balance of the water flow, making the water moment act on the guide vanes and blades at different circumferential positions. This case, in turn, causes the adjustment of the guide vane opening and the blade rotation angle. Asynchrony, the occurrence of synergy deviation, further exacerbates the hydraulic imbalance, resulting in increased vibration [20].

The above phenomena occurring during the operation of the low-head tubular turbine cannot be presented in the model test [21]. Thus, the traditional research method ignores the influence of the fluctuation of the free surface and the water gravity in the reservoir area. The traditional method cannot accurately reflect the actual situation of the tubular turbine. Thus, a big difference exists between the operating performance of the turbine and the expected target of the designer. Table 1 shows its model machine and prototype machine parameters taking a power station as an example. Then, Figure 1 depicts the water head (H) and the runner diameter (D_1).

Table 1. Parametercomparison between the model machine and prototype machine of a tubular power station.

	Model Machine	Prototype Machine
D_1 (m)	0.34	7.5
H (m)	3	2.5
H/D_1	8.82	0.33
Hydrostatic pressure difference in the runner chamber ΔP (Pa)	Pg × 0.34	Pg × 7.5

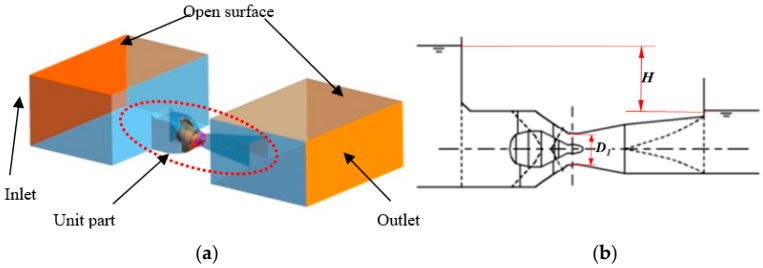

Figure 1. Geometric model. (**a**) Computational domain; (**b**) diagram of water head (H) and runner diameter (D_1).

For the flow of the model to be similar to the prototype, the similar criteria number must be equal. However, the water head of the tubular turbine is low, and the experimental water head cannot be reduced proportionally during the model test. Moreover, the H/D_1 of the above-mentioned power plant model machine is 26.7 times that of the prototype machine. Then, the hydrostatic pressure difference $\rho g D_{1m}$ in the model runner chambers is only 4.5% of the hydrostatic pressure difference $\rho g D_{1p}$ in the prototype runner. This result shows that the model machine and the prototype machine fail to meet similar conditions. Moreover, the tubular turbine has a short distance from the upstream and downstream reservoir areas, which is a typical flow including the open channel part. Therefore, the water flow of the model and the prototype is required to be similar under the action of gravity to satisfy the Froude similarity criterion. In addition, the scale of physical quantities between the model and the prototype is also constrained by this criterion. However, the difference between the gravitational acceleration of the model and the prototype is very small, and g_p is approximately considered to be equal to g_m. If the flow of the model is similar to that of the prototype, then the parameters such as the velocity scale, flow scale, time scale, acceleration scale, and pressure scale must all be a specific value, making it more difficult to implement. In addition, the influence of the fluctuation of the free surface in the reservoir area and the water gravity on the flow characteristics in the turbine cannot be reflected in the model test. Therefore, the severe vibration and noise generated during the operation of the low-head tubular turbine cannot be accurately known by the model machine. With the increase in the size and capacity of the ultra-low-head tubular turbine, the above phenomenon becomes more prominent and becomes an important factor restricting the stable operation of the low-head tubular turbine. At present, the influence of free surface and gravity on the internal flow of the tubular turbine has attracted the attention of relevant scholars. The relevant literature showed that gravity has an important influence on the dynamic stress characteristics of the cavitation performance of the horizontal tubular turbine [22,23]. Furthermore, the dynamic fluctuation of the free surface [24,25] makes the force on the runner blade of the tidal tubular turbine fluctuate greatly.

In view of the above situation, based on the numerical calculation model of prototype machine performance that fully considers the free surface in the reservoir area and water gravity, this research conducts a numerical study on the machine performance of tubular turbines with different H/D_1. The study also deeply analyzes the internal transient flow characteristics and water pressure pulsation characteristics of the tubular turbine with different H/D_1. Moreover, the influence law of free surface and water gravity on prototype tubular turbines with different H/D_1 is revealed. These research results provide a theoretical basis for the hydraulic design and stable operation of the tubular turbine.

2. Materials and Methods

Any complex flow process in nature can be described by continuity equation, momentum conservation equation, and energy conservation equation. The flow in the turbine is a three-dimensional unsteady flow with water as the medium. Water is generally considered an incompressible fluid, and the heat exchange amount is very small, and thus energy conservation can be ignored. Therefore, the complex three-dimensional viscous incompressible flow in the turbine can be obtained from the following two equations to describe:

(1) Continuity equation

$$\frac{\partial \rho}{\partial \mathrm{t}} + \frac{\partial}{\partial x_i}(u_i) = 0 \tag{1}$$

(2) Momentum equation

$$\frac{\partial}{\partial t}(\rho u_i) + \frac{\partial}{\partial x_j}(\rho u_i u_j) = -\frac{\partial p}{\partial x_i} + \frac{\partial}{\partial x_j}\left(\mu \frac{\partial u_i}{\partial x_j} + \tau_{ij}\right) + S_i \tag{2}$$

where ρ is the density of fluid, τ_{ij} is the shear stress of fluid, μ is the viscosity coefficient of fluid, and u is the velocity vector of fluid.

The water flow direction of the horizontal unit is perpendicular to the direction of gravity. Hence, the influence of the gravity factor on the internal flow field of the turbine needs to be considered in the numerical calculation; thus the source term in the equation is defined as $S_i = \rho g$.

The flow simulation with the free surface focuses on how to track the free surface. The problem can be solved in many ways, such as the steel lid law, marking particle method, the height function method, and the volume of fluid (VOF) method. The advantage of the VOF method is that it is the only function that can describe a variety of complex changes in the free surface. Thus, in this study, the VOF method is used to solve the water–air two-phase flow in the bulb turbine while considering the free surface. The position of the free surface is determined by establishing and solving the transport and diffusion equation of the volume function.

The transport and diffusion equation of the volume function is as follows:

$$\frac{\partial \propto_q}{\partial t} + u_q \frac{\partial \propto_q}{\partial x_q} = 0, \tag{3}$$

where $\propto_q$ is the volume fraction of the q-th phase fluid in the control body.

When $\propto_q = 0$, the q-th phase fluid does not exist in the control body.

When $\propto_q = 1$, the control body is filled with the q-th phase fluid.

When $0 < \propto_q < 1$, the q-th phase fluid and other phase fluids exist in the control body simultaneously, and the phase interface is clear.

Therefore, according to the local fluid volume fraction, each control unit in the computational domain is assigned variable values and physical properties. By solving the VOF equation, the volume fraction of each phase in each control unit can be obtained, combined with the phase volume fraction of nearby cells, and according to certain rules, the phase boundary can be accurately described, and then, the control equation can be solved discretely.

As the standard k-ε turbulence model has the characteristics of stability, simplicity, and economy, this model has sufficient accuracy in a wide range of applications, including boundary layer flow, flow in pipes, and shear flow. Therefore, in this study, the standard k-ε turbulence model with simple, stable, and relatively high economy and accuracy is adopted. The SIMPLE Calgorithm with better convergence in the actual calculation is combined to solve the complex three-dimensional incompressible flow in the turbine.

3. Results

This study mainly examines the performance of the prototype tubular turbine under the influence of free surface and water gravity, which is consistent with the actual situation. Figure 1 shows the selected computational domain (including the upstream and downstream reservoir areas and the tubular turbine).

This study aims to study the distribution law of the flow parameters in the tubular turbine under different H/D_1 conditions and to explore the relationship between the distribution law of the flow parameters and H/D_1. Thus, different actual hydropower turbines under different water heads and with five-, four-, three-, and two-blade runners are selected as the research objects. Table 2 shows the basic parameters for each actual hydropower turbine.

High-quality structured grids for all components of the turbine units are created by using the commercial software ANSYS ICEM-CFD with multi-block templates. Considering the large density difference between water and vapor, the phase interface is often clear at the free surface. Moreover, sparse grids near the free surface will cause a wider phase interface and a greater error in the results; thus dense grids are needed near the free surface. Meanwhile, the volume fraction gradient of the water and vapor changes largely at the phase interface; denser grids can help the better development between the water

phase and the vapor phase. In addition, owing to the complex flow components of the tubular turbine, its internal flow patterns are also complex. To accurately capture the complex flow in the bulb section, guide vane, runner, and draft tube section of the tubular turbine, these components require a more refined grid distribution. The upstream and downstream reservoir areas are larger in size, and the flow is relatively stable, and thusthe grid distribution is relatively sparse. This method can not only prevent the calculation speed slowdown caused by the dense grids of the entire computational domain effectively but also make a good simulation for the phase interface and complex flow state.

Table 2. Basic parameters of the tubular turbine at different heads.

Numberof Blades	Number of Guide Vanes	Hub Ratio	Water Head (m)	Runner Diameter (m)	Rotating Speed (r/min)	H/D_1
5	16	0.41	19	5.1	115.4	3.73
4	16	0.36	10.2	6.7	75	1.52
3	16	0.34	9	7.2	75	1.25
2	16	0.3	4.3	7.6	60	0.57

To reduce the influence of the number of grids on the numerical calculation results, taking the three-blade turbine as an example, the average static pressure on the blade surface is selected as the evaluation value to verify the mesh independence, as shown in Figure 2. When the number of grids in the computational domain is greater than or equal to 3.14 million, the static pressure value of the blade surface remains unchanged. Therefore, the grid distribution with a computational grid number of 3.14 million is finally selected as the calculation grid. The bulb section, guide vane, and draft tube use the same mesh number. Moreover, the runner adopts the same mesh topology structure when the number of blades is different, and the number of generated meshes varies with the number of blades. Table 3 presents the specific grid distribution of each part, and Figure 3 shows the grid distribution of the computational domain.

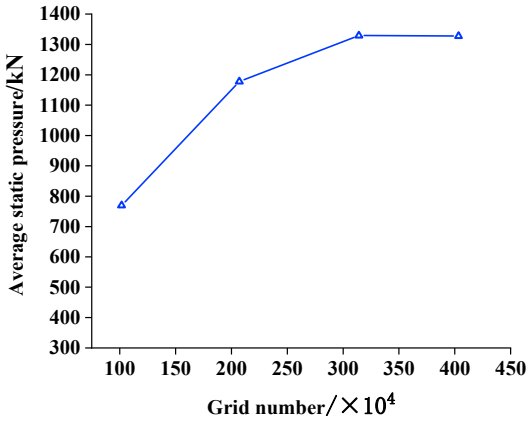

Figure 2. Grid independence verification.

Table 3. Grid number of each flow component.

Turbine Flow Parts	Nodes	Grid Numbers
Upstream reservoir area and diversion section	668,275	667,168
Guide vane	1,087,760	1,017,042
Draft tube and downstream reservoir area	391,208	404,160
Five-blade runner	1,847,738	1,699,093
Four-blade runner	1,478,185	1,359,274
Three-blade runner	1,108,630	1,019,456
Two-blade runner	950,086	909,637

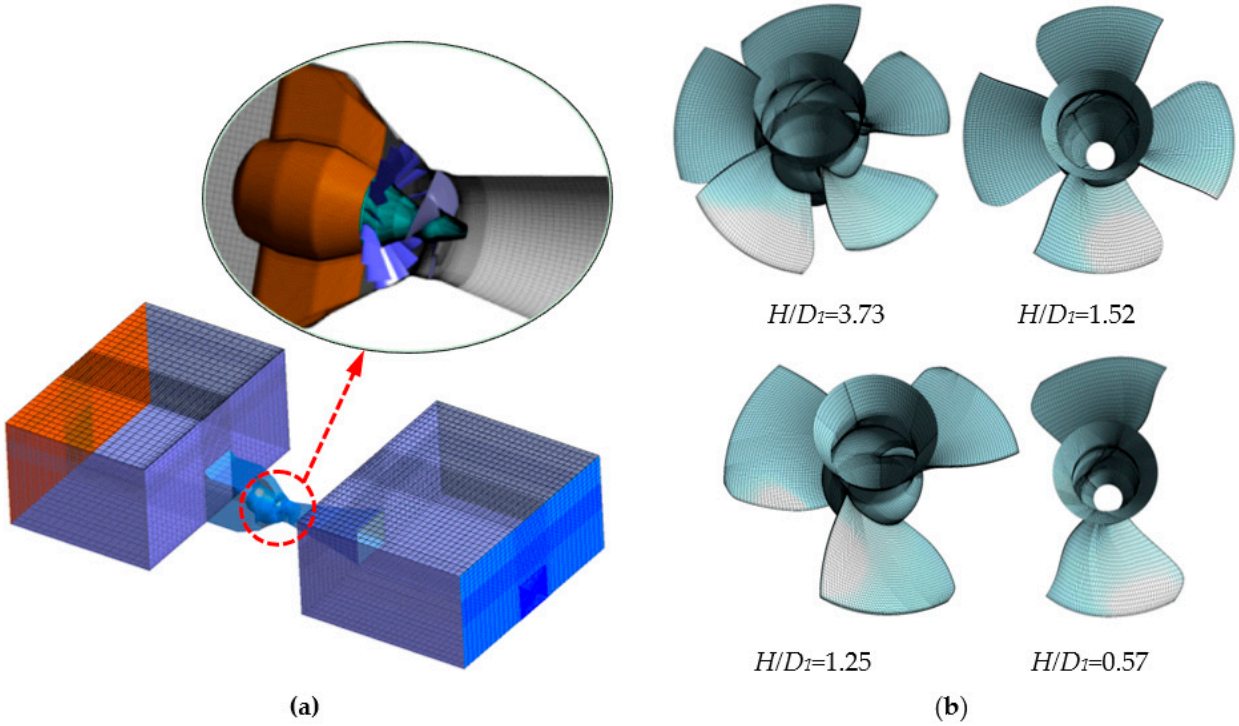

Figure 3. Grid distribution of computational domain. (**a**) The overall grid distribution of the computational domain; (**b**) grid distribution of the runner with different numbers of the blade.

Figure 4 showsthe initial flow field in this study.The red region indicates the initial position of the water, and the blue region indicates the initial position of the air. Boundary conditions are set as follows:

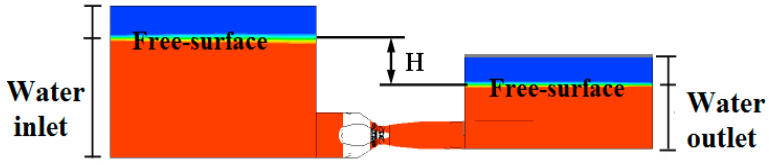

Figure 4. Boundary conditions and initial flow field.

Inlet of the upstream reservoir: liquid height and hydrostatic pressure.
Outlet of downstream reservoir: liquid height and hydrostatic pressure.
The top of reservoir: opening surface (air inlet; the water volume fraction is 0).
Rotating components: the runner is the rotating component, and the rotating speed is given.
Solid wall: solid wall with smooth no-slip boundary.
Medium: water and air.

4. Experimental Verification of Numerical Calculation Method

For a tubular turbine, meeting geometric similarity and flow similarity in model testsis difficult, and directly conducting research on prototype machinesis not easy. Thus, numerical simulation becomes the best method for the performance research of prototype tubular turbines, and the feasible and reliable numerical simulation method is the key to the success of numerical research. However, testing is difficult because of the inability to arrange the measuring points on the unit and the lack of suitable measuring instruments to accurately measure the flow velocity distribution and pressure distribution of the section.Therefore, this study simplifies the tubular unit into a pressure pipeline containing upstream and downstream water tanks for experimental research, as shown in Figure 5. The experimental

model is designed according to the gravity similarity criterion. Figure 6 depicts the model test and the arrangement of measuring points; the geometric scale is 1:50. Moreover, Table 4 presents the other corresponding physical quantity scales. At the same time, the numerical simulation considering the free surface and water gravity forthe pressure pipeline model is carried out.

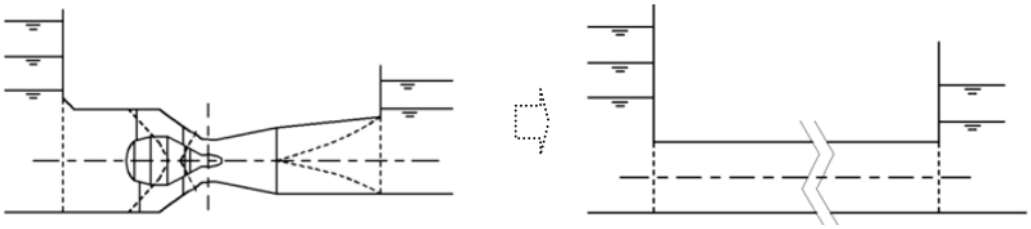

Figure 5. Simplification of the model.

(**a**) (**b**) (**c**) (**d**)

Figure 6. Test model. (**a**) Pressure pipe; (**b**) upstream reservoir; (**c**) distribution of pressure measuring points; (**d**) draft tube.

Table 4. Physical scale of the experimental mode.

Name	Formula	Value
Geometric scale	$\lambda_L = l_p/l_m$	50
Speed scale	$\lambda_V = \lambda_L^{0.5}$	7.071
Flow scale	$\lambda_Q = \lambda_L^{2.5}$	17,678
Pressure scale	$\lambda_P = \lambda_L$	50
Time scale	$\lambda_t = \lambda_L^{0.5}$	7.071
Roughness scale	$\lambda_n = \lambda_L^{1/6}$	1.919

Figures 7 and 8 show the comparison of the pressure and flow velocity in the pressure pipeline model obtained through numerical simulations and experiments, respectively. From the figure, the flow state in the pressure pipeline obtained through the numerical research method considering the free surface and water gravity is similar to the experimental results. Moreover, the feasibility of analyzing the flow characteristics of a tubular turbine considering free surface and water gravity by the numerical research method is further verified. Therefore, this numerical simulation method considering the free surface in the reservoir area and water gravity can be used to estimate the performance of the horizontal tubular unit.

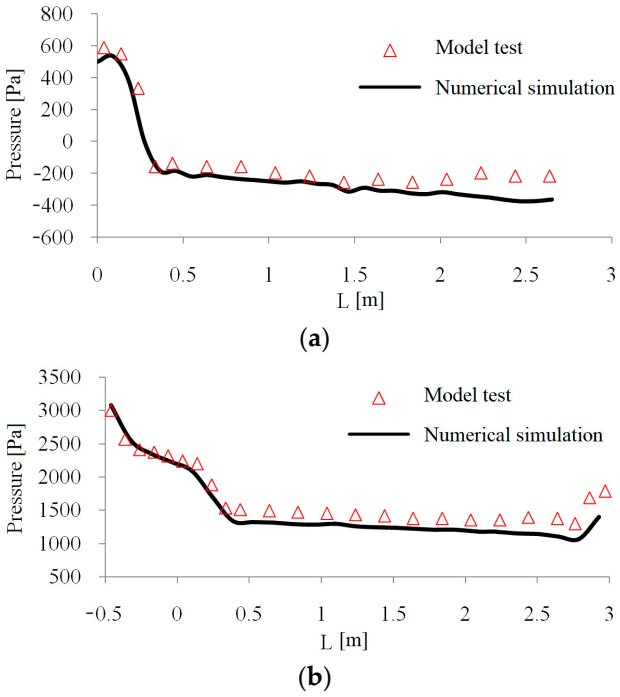

Figure 7. Pressure distribution at the bottom and top of the pipeline. (**a**) Top of pressure pipe; (**b**) bottom of pressurized pipe.

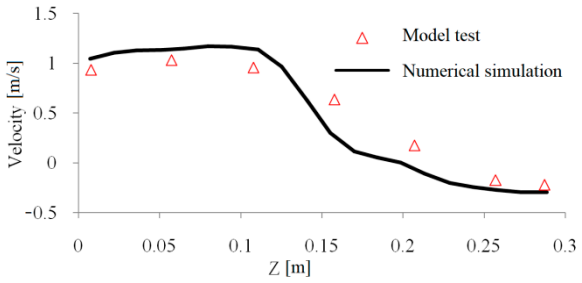

Figure 8. Pipeline inlet velocity distribution.

5. Analysis and Discussion of Calculation Results

5.1. Analysis of the Internal Flow Field Characteristics of the Tubular Turbine with Different Head Sections

Figure 9 shows the pressure distribution inside the unit under different H/D_1. In the entire calculation domain, the pressure above the free surface is constant at atmospheric pressure. Below the free surface, the pressure of the runner part fluctuates because of the output power when the runner rotates. Furthermore, the pressure in the rest flow parts increases with the increase inwater depth. The pressure in the upstream channel of the runner is determined by the water depth of the upstream reservoir area. Moreover, the pressure of the downstream channel of the runner is determined by the water depth of the downstream reservoir area. The reason is that the water head of the turbine is the difference between the upstream and downstream water levels. This water level difference is also the energy that the runner needs to convert; thusit also indirectly reflects the pressure difference before and after the runner.When H/D_1 is large, the upstream water level is deep, and the downstream water level is shallow, and thusthe pressure changes before and after the runner are evident. When H/D_1 is small, a small difference between the upstream and downstream water levels makes the pressure change before and after the runner smaller.

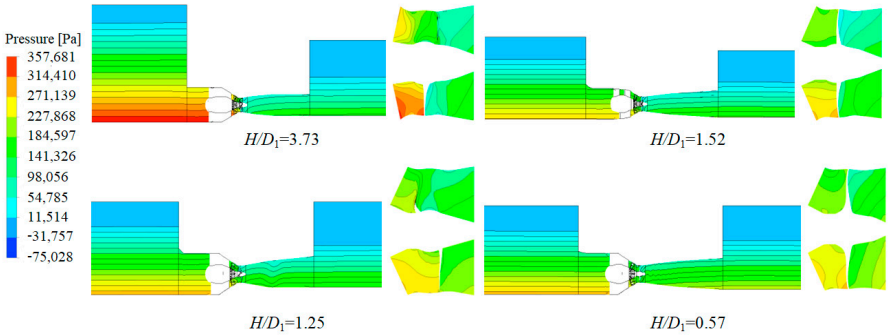

Figure 9. Pressure distribution in the flow channel.

To compare the speed distribution in the tubular turbine under different H/D_1 conditions, the relative velocity C_v is introduced:

$$C_v = \sum \frac{Av_i}{Q} \tag{4}$$

where A is the flow area, Q is the flow rate, and v_i is the instantaneous speed of the water flow.

In order to analyze the flow state of different parts inside the turbine in detail, corresponding measuring points and observation planes are arranged inside the turbine. As shown in Figure 10.

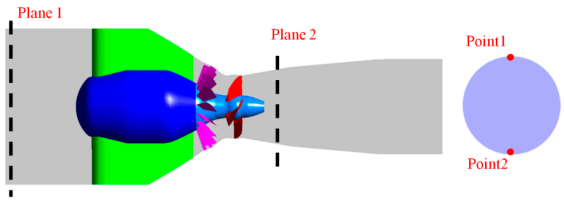

Figure 10. Schematic diagram of measuring point layout and observation plane position.

Figure 11 shows the relative velocity distribution at the inlet of the unit (Plane 1 of Figure 10) at different H/D_1. From the figure, in most of the areas of the inlet, the non-uniformity of the flow velocity distribution at the inlet of different H/D_1 units is different. This non-uniformity is more evident along the direction of the inlet height. To be more intuitive and quantify this inhomogeneity, the relative velocity from the top to the bottom of the middle position of the inlet section is taken, as shown in Figure 12. From the figure, when H/D_1 is large, the uniformity of the flow velocity distribution along the height direction is better. Moreover, when H/D_1 = 0.57, the difference between the maximum relative flow velocity and the average value at the middle position of the inlet section is up to 0.163, whereas the remaining three H/D_1 cases have only 0.071, 0.052, and 0.061, respectively. The small H/D_1 aggravates the non-uniformity of the incoming flow of the unit, and thus the flow entering the unit is more concentrated at the top of the inlet section.

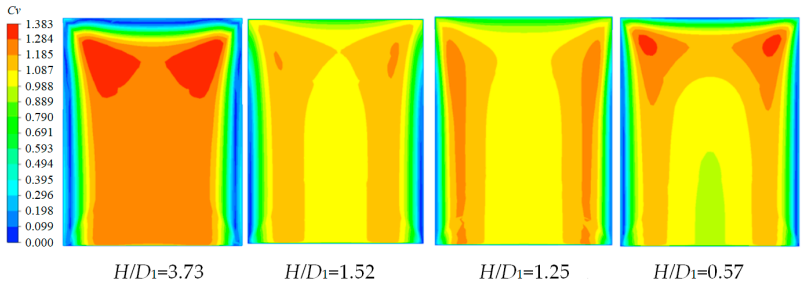

Figure 11. Relative velocity distribution of the turbine inlet.

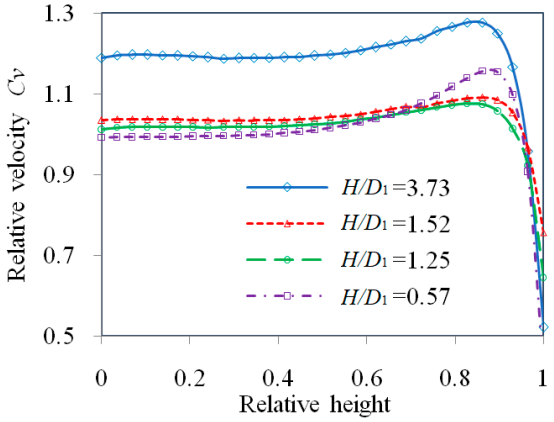

Figure 12. Relative velocity distribution at the middle line of the turbine inlet.

Figure 13 shows the relative velocity distribution at different positions along the circumferential direction before the guide vane inlet at different H/D_1. It can be seen from the figure that with the decrease in H/D_1, the uniformity of the flow velocity distribution along the height direction of the guide vane is better. Along the circumferential direction, owing to the shunt effect of the bulb body and the upper and lower shafts on the flow, before reaching the movable guide vane, a small flow velocity area still exists near the end of the shaft. In addition, the flow velocity distribution near the bulb body is the most uneven. When passing through the guide vanes, the water flow is further equalized by the guide vanes. The uneven distribution of flow velocity in a small area caused by the vertical shaft before the entrance of the guide vanes has been further improved. However, unevenness still exists, as shown in Figure 14.

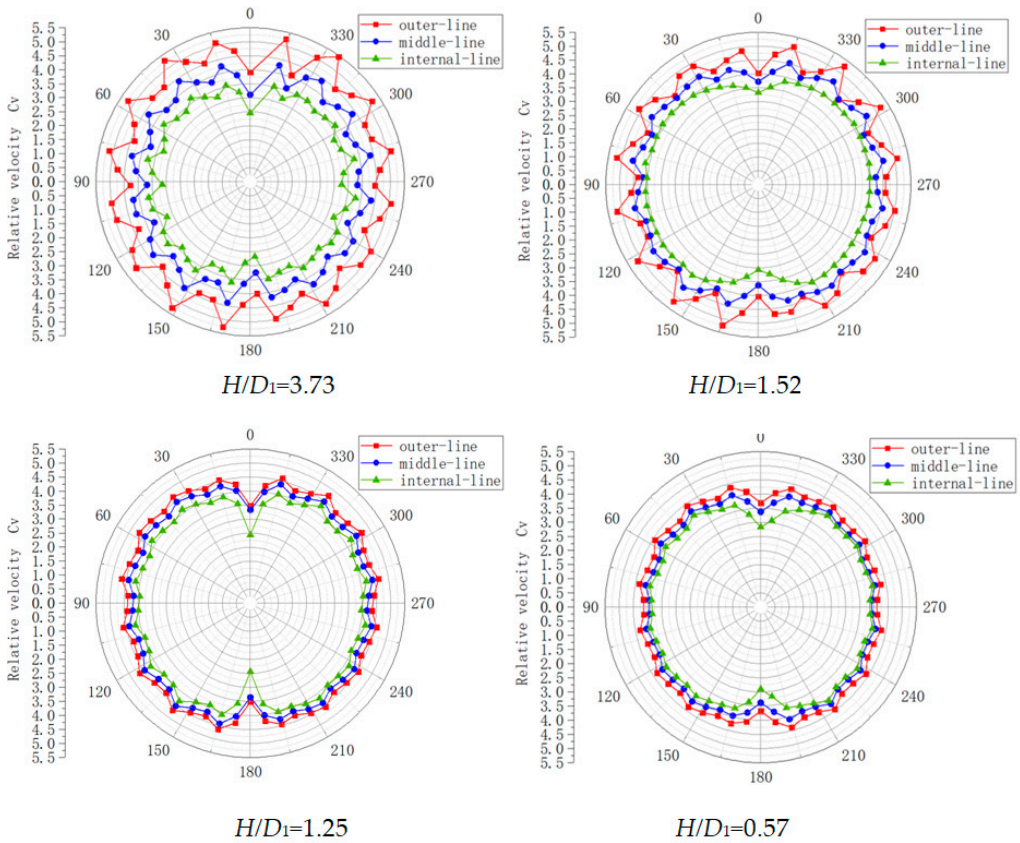

Figure 13. Relative velocity distribution of the guide vane inlet.

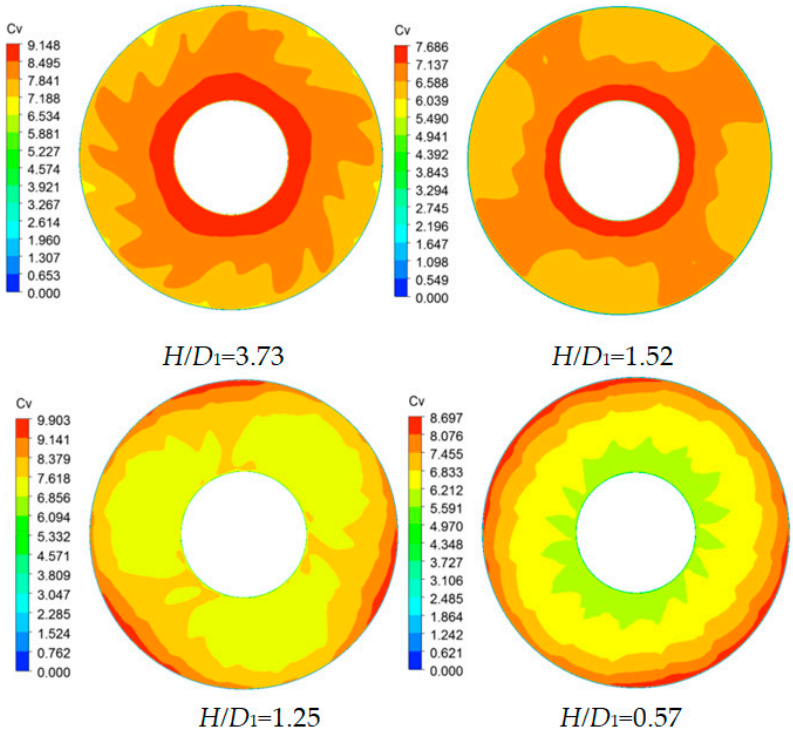

Figure 14. Relative velocity distribution of the runner inlet.

5.2. Analysis of the Internal Pressure Pulsation Characteristics of the Tubular Turbine with Different Head Sections

During the actual operation of the tubular turbine, the pressure on the blade at different positions is different because of the influence of the hydrostatic pressure caused by the water gravity. During the operation of the turbine, the blade will experience a pressure cycle process behaving as "high pressure–low pressure–high pressure." To study the different effects of the hydrostatic pressure generated by the water gravity on the water pressure distribution on the blade surface under different H/D_1 conditions in detail, four monitoring points on the blade (Figure 15) were selected to conduct the transient state analysis of the blade surface pressure pulsation. Figure 16 shows the pressure coefficient Cp ($Cp = P/\rho gH$) fluctuation on the blade under different H/D_1. From the figure, under different H/D_1 conditions, the pressure distribution on the blade surface changes periodically during the operation of the horizontal tubular turbine. The vertical displacement experienced by the part of the blade near the shroud is close to the runner diameter D_1. Thus, the hydrostatic pressure change experienced is $\rho g D_1$. The vertical displacement experienced by the part of the blade near the hub is close to the hub diameter d_b; thusthe hydrostatic pressure change experienced is $\rho g d_b$. Moreover, the pressure change on the blade surface is the joint action of the hydrostatic pressure and the dynamic water pressure. Furthermore, the dynamic water pressure on the blade surface changes less with height, and the change law of the pressure fluctuation is mainly dominated by the hydrostatic pressure. Therefore, the magnitude of the pressure fluctuation on the blade near the shroud is greater than that near the hub. As H/D_1 decreases, the submerged depth of the runner increases, and the hydrostatic pressure difference from the top to the bottom of the runner chamber increases. When the blade makes one revolution, the fluctuation amplitude of the pressure at different positions on the blade increases significantly. Tubular turbine blades are prone to vibration under the action of this unbalanced periodic pressure fluctuation, and even material fatigue damage occurs. Particularly in the case of ultra-low H/D_1, the vibration of the tubular turbine is more severe, and this phenomenon is more consistent with the actual operation of the power station.

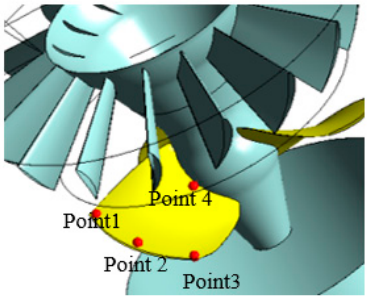

Figure 15. Pressure monitoring location.

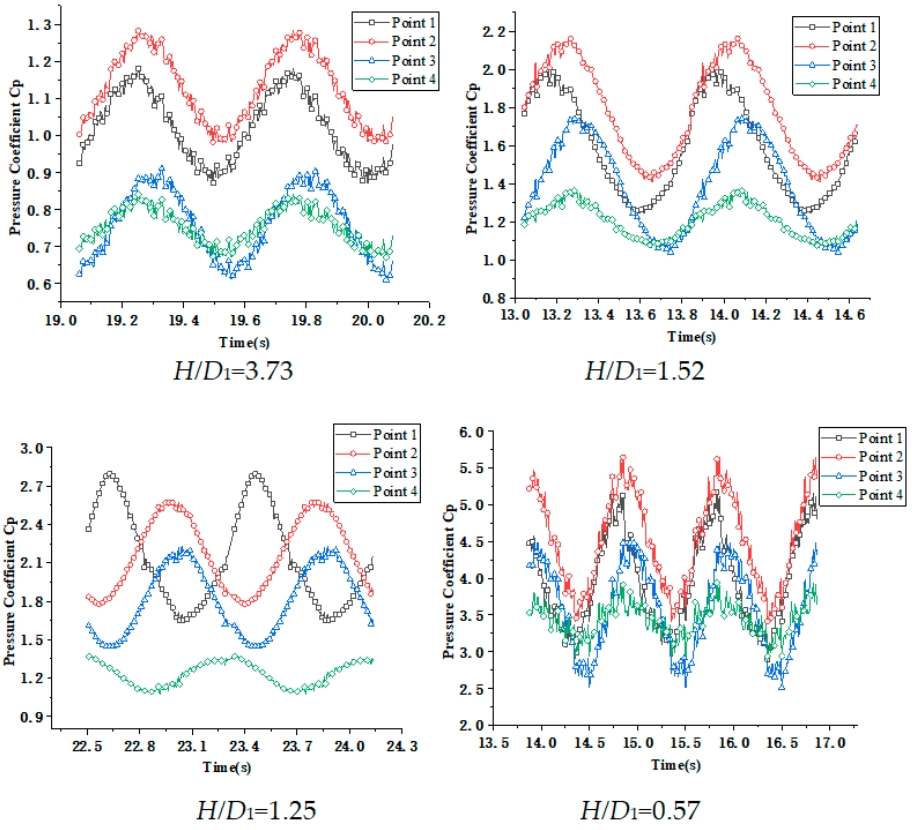

Figure 16. Pressure variation on the blade of different H/D_1 during rotating.

To analyze the pressure pulsation in the draft tube of the tubular turbine with different H/D_1, two monitoring points above and below the inlet section of the draft tube are selected, as shown in Figure 10. Figure 17 shows the variation curve of the pressure with time at each monitoring point and its frequency spectrum characteristics. From Figure 17, the frequency of pressure pulsation in the draft tube is relatively complex, but for the same unit, the pressure pulsation and frequency spectrum characteristics at the top and bottom of the draft tube have the same law. The pressure difference between the two monitoring points at the same time is the static pressure difference caused by the elevation difference. Moreover, the frequency characteristics are the same except for the difference in amplitude. The draft tube has a typical low-frequency pressure pulsation under different H/D_1 with frequencies of 1.87, 1.256, 0.706, and 1.956Hz. When the water head is high (H/D_1 = 3.73), the pressure pulsation in the draft tube is mainly dominated by low-frequency pressure pulsation. However, with the decrease inthe water head, when the H/D_1 is 1.52, 1.25, and 0.57, respectively, the pressure pulsation is very complex, and the high-frequency pressure pulsation signals with a frequency of 1500 to 2300 Hz appear concentrated. Furthermore, the amplitude of the pressure pulsation of each frequency in the draft tube increases with

the decrease inthe H/D_1. The smaller the H/D_1, the more severe the hydraulic vibration caused by the pressure pulsation in the draft tube, which will have a great impact on the stability of the turbine.

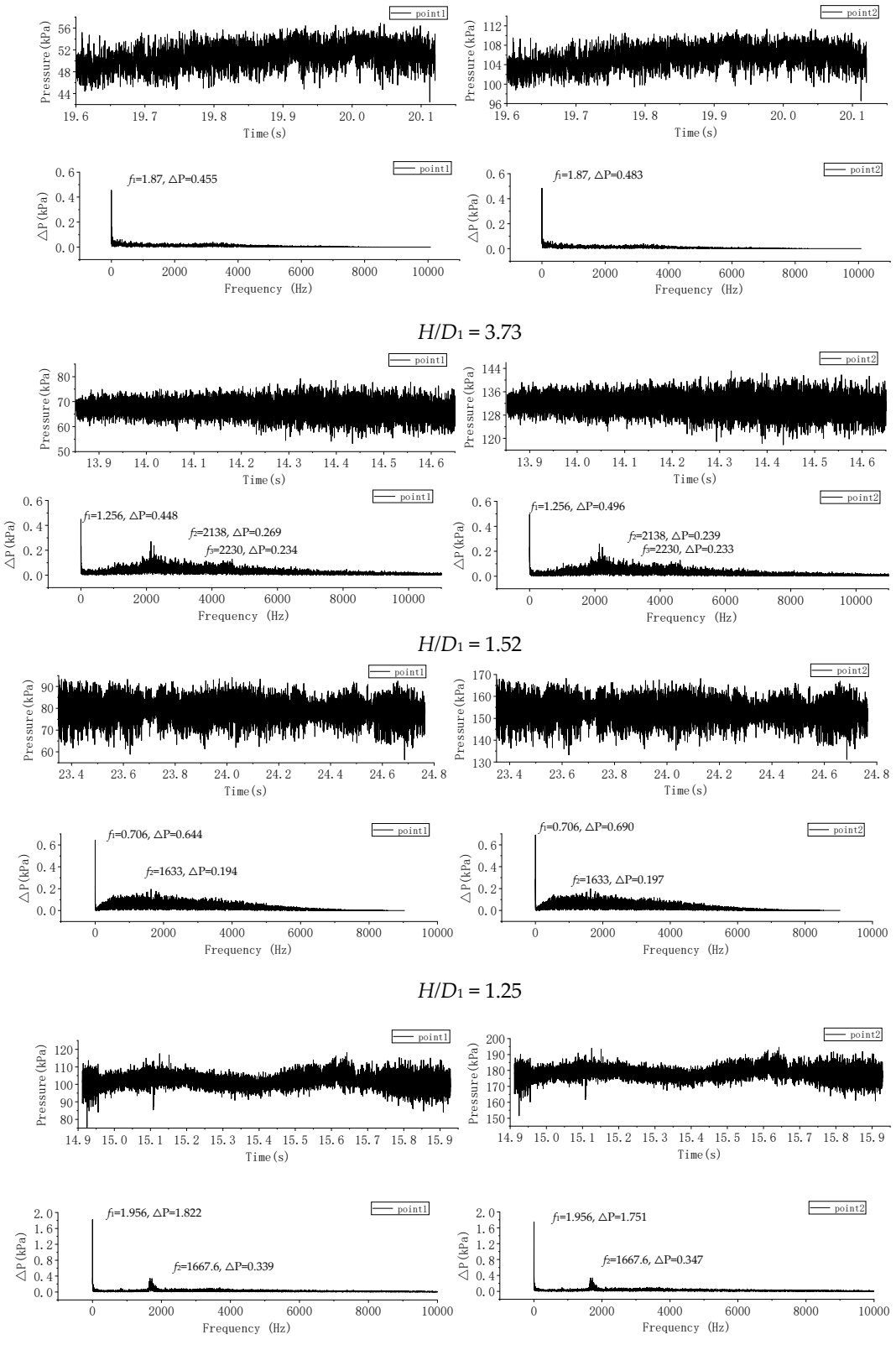

Figure 17. Characteristic distribution of pressure pulsation in the draft tube.

5.3. Analysis of Torque Characteristics of the Tubular Turbine with Different Head Sections

To facilitate the analysis of the torque on the blades at different positions of the runner, the torque percentage is introduced, and its expression is shown in Equation (5), where M_i is the torque value of a single blade, and i is the blade number.

$$\text{Torque percentage} = \left(\frac{M_i}{\sum M_i}\right) \times 100\% \quad (5)$$

Figure 18 shows the torque at different H/D_1 generated by the blades in different positions. The average value of the torque percentage of each blade is used as a reference value. The average value is defined as follows: the torque suffered by the entire runner is recorded as 100%. When the free surface and water gravity are not considered, the torque suffered by each blade is the same, and the average torque percentage of each blade is 100/N (%), where N is the number of blades.

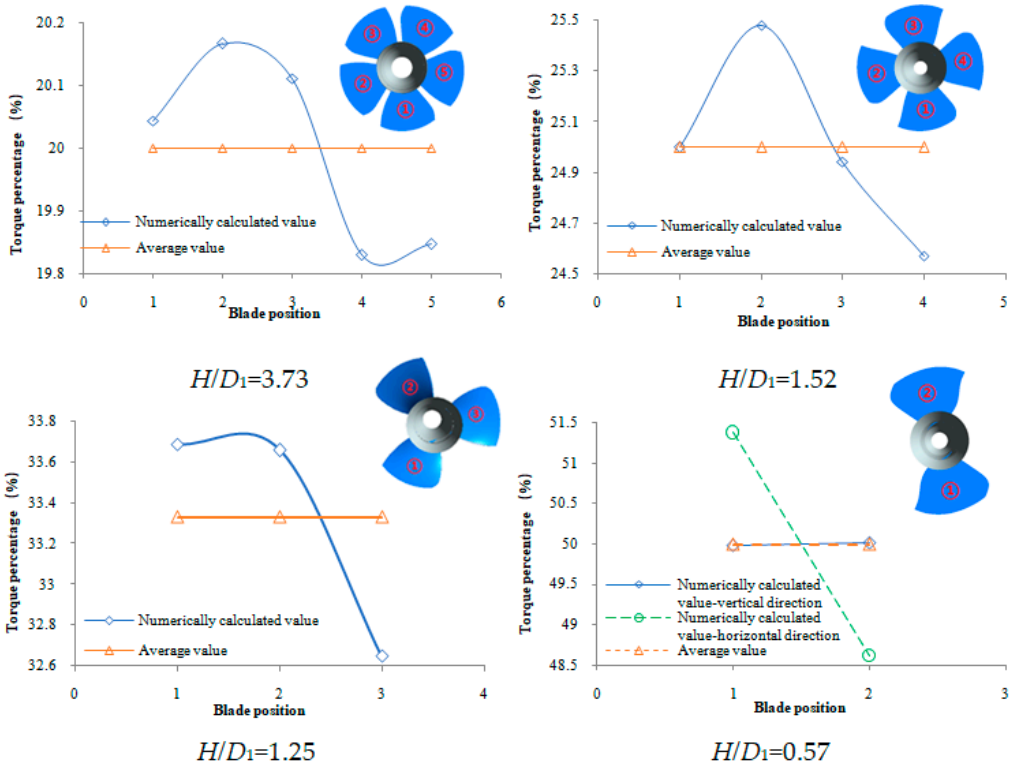

Figure 18. Torque for different blades.

When considering the free surface and water gravity, Figure 18 shows that when the H/D_1 is different, the blade torque at different positions deviates from the average value. When the blade starts to rotate around the shaft from the bottom of the runner chamber, the change process of torque is as follows: during the rotation of the blade from the bottom to the top of the runner chamber, the torque increases from the average value to the maximum value and then gradually decreases to the average value; when the blade rotates from the top to the bottom of the runner chamber, the torque starts to decrease from the average value to the minimum value and then gradually increases to the average value. The maximum and minimum torque of the blade mainly occurs at the horizontal position, and the position where the torque is close to the average value is the top and bottom of the runner chamber. Therefore, when the runner rotates, the maximum torque always occurs when the blade rotates against the water gravity. Moreover, the minimum value always occurs in the process of the water flow gravity pushing the blade rotation. Each blade bears the fluctuation of the torque when the runner rotates.

Table 5 shows the variation of the blade torque relative to the average value for different H/D_1. From the table, the influence of free surface and water gravity on blade torque varies with H/D_1 and the number of blades. The smaller the H/D_1 is, the lowerthe number of blades is, and the greater the torque fluctuation is, which is not conducive to the safe and stable operation of the turbine. Therefore, when a two-blade runner is used in an ultra-low-head power station, although a small number of blades can maximize the overflow of the turbine, problems such as the increase inblade area and the large fluctuation of torque are unfavorable to the safe and stable operation of the power station.

Table 5. Relative variation of torque.

H/D_1	Torque Increase Value	Torque Reduction Value
3.73	+0.83	−0.85
1.52	+1.293	−1.706
1.25	+1.802	−2.056
0.57	+2.75	−2.75

6. Conclusions

In this study, a numerical study on the prototype tubular turbine with different H/D_1 is carried out under the consideration of the free surface in the upstream and downstream reservoir areasand water gravity. The distribution and development law of different hydraulic elements in the prototype tubular turbine during the operation are analyzed; the main conclusions are as follows:

(1) Owingto the short water diversion section of the tubular turbine, the water flow from the reservoir area to the inlet section undergoes a sudden change in the flow channel, which makes the axial symmetry of the flow velocity distribution poor, and the lower the H/D_1, the more evidentthis phenomenon is. Although the bulb body and the guide vane have an apparent equalizing effect on the water flow, the axisymmetric of the water flow along the circumferential direction before reaching the runner is still poor.

(2) Periodic pressure fluctuations will appear on the blade when the runner rotates. The smaller the H/D_1 is, the submerged depth of the runner increases, and the amplitude of the water pressure fluctuation on the blade increases significantly. Under the action of this unbalanced periodic pressure fluctuation, the blade of the tubular turbine is prone to vibration and even material fatigue damage.

(3) Under different H/D_1, a low-frequency, high-amplitude pressure pulsation occurs in the draft tube. The amplitude of this low-frequency pressure pulsation increases with the decrease in H/D_1. Moreover, when H/D_1 decreases, the high-frequency pressure pulsation signal with a concentrated frequency appears in the draft tube, which will cause the hydraulic vibration of the low-head turbine.

(4) During the rotation of the runner, the torque of a single blade will fluctuate periodically. The maximum torque appears at the horizontal position of the runner and in the process of overcoming the water gravity. Moreover, the minimum value appears at the horizontal position of the blade, whereasthe water gravity pushes the blade to rotate. With the blades at the top and bottom of the runner chamber, the torque is close to the average blade. The fluctuation of blade torque becomes stronger with the decrease in H/D_1, which is not conducive to the stability of the output of the turbine.

It can be seen from the research results that for a horizontal tubular turbine, the submerged depth of the runner increases with the decrease inthe water head, the unbalanced hydrostatic pressure caused by water gravity from top to bottom in the runner chamber makes the hydraulic imbalance and hydraulic vibration inside the turbine, as well as the fluctuation of the output, more severe. This conclusion can well reveal the reasons for the unstable output and severe vibration of the tubular turbine during operation at the ultra-low water head. Severe vibration will inevitably cause fatigue damage tomaterials

and affect the life of the unit.Therefore, in the next stage of the research, the fluid-structure coupling analysis of the prototype tubular turbine can be carried out to reveal the stress–strain characteristics of the tubular turbine runner blade and provide effective guidance for the hydraulic design and operation of the tubular turbine.

Author Contributions: Y.Z. and M.D. carried out the numerical simulations, analyzed data, conducted the experiment, and wrote the first draft of the manuscript. J.F. and Z.L. conceived and supervised the study and edited the manuscript. X.L. edited the manuscript. All authors have read and agreed to the published version of the manuscript.

Funding: This research was funded by the National Natural Science Foundation of China, grant numbers 52009105 and 52079108.

Institutional Review Board Statement: Not applicable.

Informed Consent Statement: Not applicable.

Data Availability Statement: Not applicable.

Conflicts of Interest: The authors declare no conflict of interest.

References

1. Avellan, F. Introduction to Cavitation in Hydraulic Machinery. In Proceedings of the 6th International Conference on Hydraulic Machinery and Hydrodynamics, Timisoara, Romania, 21–22 October 2004; University of Timişoara: Timisoara, Romania, 2004.
2. Zhang, Y.; Liu, M.; Wu, Y.; Lin, P. Effect of Tip Clearance on Cavitation Flow of Tubular Tubular Turbine. *J. South China Univ. Technol. (Nat. Sci. Ed.)* **2018**, *46*, 58–66.
3. Li, G.; Lu, C. Experimental study on cavitation characteristics of Tubular turbine blades. *J. Hydroelectr. Eng.* **2017**, *36*, 102–109.
4. Jósefsson, V.A. Flow Analysis of a Rotating Tidal Turbine Blade Using a Dynamic Mesh. Master's Thesis, University of Iceland, Reykjavík, Iceland, 2011.
5. Benigni, H.; Jaberg, H. Stationary and Transient Numerical Simulation of a Tubular Turbine. In Proceedings of the 5th IASME/WSEAS International Conference on Fluid Mechanics and Aerodynamics, Athens, Greece, 25–27 August 2007.
6. Wang, Z.; Zhou, L.; Chen, Y. Hydraulic Loss Analysis in Tubular Turbine. *Large Electr. Mach. Hydraul. Turbine* **2004**, *5*, 40–43.
7. Yaseen, Z.M.; Ameen, A.M.S.; Aldlemy, M.S.; Ali, M.; Afan, H.A.; Zhu, S.; Al-Janabi, A.M.S.; Al-Ansari, N.; Tiyasha, T.; Tao, H. State-of-the Art-Powerhouse, Dam Structure, and Turbine Operation and Vibrations. *Sustainability* **2020**, *12*, 1676. [CrossRef]
8. Tas, Y.; Kahraman, G.G. Crack failure in hydrodynamically lubricated bearings: A case study hydraulic turbine. *Eng. Fail. Anal.* **2021**, *121*, 105123.
9. Valentín, D.; Presas, A.; Bossio, M.; Egusquiza, M.; Egusquiza, E.; Valero, C. Feasibility of Detecting Natural Frequencies of Hydraulic Turbines While in Operation, Using Strain Gauges. *Sensors* **2018**, *18*, 174. [CrossRef] [PubMed]
10. Liang, W.; Huang, H.; Wu, Z.; Dong, W.; Yan, X.; Liu, Y. Numerical simulation of fluid-solid coupling of a Francis turbine with an upper crown cavity. *J. Hydraul. Eng.* **2020**, *51*, 1383–1392, 1400.
11. Zhang, F.; Zheng, Y.; Wei, J.; Ding, L.; Yang, C. Analysis of Runner Crack Retrofit of Francis Turbine Based on Fluid-Solid Coupling. *J. Hydroelectr. Eng.* **2014**, *33*, 267–273. (In Chinese)
12. Kuppuswamy, N.; Rudramoorthy, R. Deformation of outer distributor cone in tubular turbine due to cavitation–A case study. *J. Sci. Ind. Res.* **2005**, *64*, 256–261.
13. Parthiban, K.P.; Vigneash, L.; Dr Kuppuswamy, N.; Dr Sridharan, P. Energy Efficient Analysis of Tubular Turbine in the Environment of Cavitation with Model Study. *IASH J.–Int. Assoc. Small Hydro* **2019**, *8*, 3–12.
14. Cheng, Q.; Zheng, L.; Wang, C. Application of two-blade runner in technical transformation of ultra-low head power station. *Sichuan Water Power* **2017**, *36*, 96–98.
15. Zhao, Y.; Li, Z.; Liao, W.; Luo, X. Numerical investigation of free surface effect on performance of tubular turbine. *J. Hydroelectr. Eng.* **2018**, *37*, 8–14.
16. Zhao, Y.; Li, Z.; Liao, W.; Zheng, X.; Luo, X. Performance Variation Study on Tubular Turbines with Different Water Head under Considering Free Surface and Water Gravity. In Proceedings of the 29th IAHR Symposium on Hydraulic Machinery and Systems, Kyoto, Japan, 16–21 September 2018.
17. Brezovec, M.; Kuzle, I.; Krpan, M.; Holjevac, N. Analysis and treatment of power oscillations in hydropower plant dubrava. *IET Renew Power Gener* **2020**, *14*, 80–89. Available online: https://digital-library.theiet.org/content/journals/10.1049/iet-rpg.2019.0523 (accessed on 15 January 2021). [CrossRef]
18. Brezoveca, M.; Kuzle, I.; Krpan, M.; Holjevac, N. Improved dynamic model of a tubular turbine-generator for analysing oscillations caused by mechanical torque disturbance on a runner blade. *Int. J. Electr. Power Energy Syst.* **2020**, *119*, 105929. [CrossRef]
19. Jošt, D. Cavitation Prediction for Water Turbines. In Proceedings of the ACCUSIM Summer School Conference, Lausanne, Switzerland, 25–28 September 2017.

20. Benišek, M.; Božić, I.; Ignjatović, B. The comparative analysis of model and prototype test results of tubular turbine. In Proceedings of the 25th IAHR Symposium on Hydraulic Machinery and Systems, Timisoara, Romania, 20–24 September 2010.
21. Zheng, C. (Translation) Size Effect of Bulb Turbine. *Hydropower* **1991**, *4*, 61–63.
22. Liu, Y.; Chang, J. Influence of gravity on flow field analysis and hydraulic performance evaluation of bulb turbine. *J. Hydraul. Eng.* **2008**, *39*, 96–102.
23. Yu, Y.; Wu, Y.; Chen, R.; Gui, S. Influence of gravity field on performance of bulb bulb turbine. *Yangtze River* **2020**, *51*, 221–224, 248.
24. Ahn, S.H.; Xiao, Y.; Wang, Z.; Zhou, X.; Luo, Y. Numerical prediction on the effect of free surface vortex on intake flow characteristics for tidal power station. *Renew. Energy* **2017**, *101*, 617–628. [CrossRef]
25. Feng, J.; Zhu, G.; Wang, Z.; Wu, G.; Luo, X. Effect of second-order Stokes nonlinear tidal wave on performance of tidal tubular turbines. *Trans. Chin. Soc. Agric. Eng.* **2019**, *35*, 48–54.